Department of Wood Engineering
University of West-Hungary
Sopron

Progress Report
No.1.

General Regularities of the Wood Surface Roughness

A new approach for wood species characterisation

Endre Magoss, PhD

Sopron
2008

Published in 2008 by the **Department of Wood Engineering, University of West Hungary, Sopron**

Printed in Sopron, Hungary
by **LŐVÉR PRINT Kht**
2008.

ISBN 978-963-9883-06-2

General Regularities of the Wood Surface Roughness

Content

Foreword

Roughness characterises the fine irregularities on a machined surface. These irregularities can be determined by measuring the height, width and shapes of the peaks and valleys produced by wood working operations and by anatomical structural properties. The surface quality is a complex definition and it is characterised today by different parameters such as the more common R_a, R_z and R_{max} parameters. Further details can be established using the Abbott-curve and its related parameters R_{pk}, R_k and R_{vk}. These parameters are standardised (DIN 4768 and 4776) and for their determination modern measuring units are commercially available.

The surface quality is depending on many influencing factors and can be related both to *wood properties* and to *machining conditions*. Among the wood properties the wood species, density, moisture content and the structural properties are to be mentioned. The structural properties include the specific number and distribution of inside diameter of tracheids and vessels, the portions of early and late wood.

The machining process has also a significant influence on the surface roughness. The most important factors are the cutting velocity and the dullness of knives, but the cutting angle of knife, the cutting angle to the grains and the vibration amplitude of machine table and work piece have also a given influence on the surface roughness.

Considerable works have been done world-wide to establish relationships between surface roughness and influencing factors and to give practical guidelines to achieve optimal machining conditions. It still remains, however, that there are many aspects of the surface roughness unknown and, therefore, generally valid relationships can not be given to describe interconnections among the many influencing factors.

One of the main difficulties is caused by fact that the wood is not a true solid material having cavities inside (vessels, cell lumens) and furthermore, the wood as a brittle material is inclined to brittle fracture. As a consequence, the cutting mechanism is always associated with local fracture of the material giving uneven surface. The cavities cut during the machining give also uneven surface. In this latter case, the surface irregularities depend on the local position of cavities relatively to the surface. Wood species with large vessels in the early wood (ring porous wood) may locally cause large surface irregularities which have nothing to do with the machining process.

At our Department, some 15 years ago, a systematic research project was launched to clear the basic regularities of the wood surface roughness. To overcome the difficulties due to the common use of wood species as a variable, a new *structure number* was introduced which uniquely characterises an arbitrary wood species in respect to its expected surface roughness component due to internal structure. The other surface roughness component due to the machining process was measured separately and the sum of these two components given the resultant surface roughness. Measurements have shown that the surface roughness will rather be determined by the internal structure of wood, especially for hard woods with big vessels. The use of structure number made it possible to establish a general relationship valid for all wood species. The effects of cutting speed, edge dullness and tooth feed on the surface roughness were also investigated and a general relationship was established including the main influencing factors. Finally, the main reasons for the relatively high standard deviation of measured roughness values were established and related to various structural properties.

I suppose so that this work is a milestone for better understanding and knowledge of wood surface roughness.

György Sitkei
Professor- Emeritus
Member of HAS

Introduction

Machined surfaces – regardless if they are made of metal, plastic or wood – are never perfectly smooth; we can observe protruding parts, valleys and peaks on them. These forms of surface irregularity are called *roughness*. Surface roughness can be caused by different factors: discontinuities in the material, various forms of brittle fracture, cavities in the texture (e.g. wood), radius of the tool edge, local deformations deriving from the free cutting mechanism.

Surface roughness usually has a primary influence on the visual appearance of materials but it might have other effects, too. Surface roughness may be extraordinarily detrimental for wood if the surface under the tool edge suffers permanent deformation. The stability of the damaged surface diminishes to a great extent; the durability of the machined surface will then be inferior.

Visual appearance and colour effects are primarily influenced by dispersion and reflection of light. An apparent example for this is transparent glass, which – following a moderate roughening process – loses transparency. The original colour of wood becomes a lot more visible if the surface is 'bright', smooth and free of irregularities. Speaking of wood, a good example in this context is ebony: the black colour gives entirely different effects depending on the surface roughness. The polished surface presents a bright black colour. A surface treated with colourless lacquer, oil or wax will lead to quite different colour effects or shades again.

The minimum surface roughness that can be achieved depends on a number of factors. Generally we can say that processing materials with bigger volume weight can result in smoother surfaces. This explains the excellent polishing ability of ebony.

Among conifer species larch has usually the biggest volume weight and accordingly it is easy to machine from the aspect of surface quality. The Tasmanian Huon pine (*Lagarostrobos franklinii*), which is lesser known in Hungary, grows extremely slowly and has an annual ring width of 0.1-0.2 mm. Its resin content is high and it can be polished excellently.

The surface roughness of wood results from multiple factors, therefore defining general rules has taken quite a long time [2, 3, 4]. New ideas in the latest decade and modern measurement techniques supported the identification of essential rules. We present here a summary of 15 years research work conducted at the University of West Hungary, Sopron, to establish the basic rules concerning the surface roughness of solid woods [5-10]. Former difficulties were lying in that the wood species, as a variable, can not be expressed in terms of numerical values. In order to solve this problem it was necessary to elaborate and introduce a new *wood structure characterisation* method. The newly defined anatomical structure number made it possible to treat all wood species in a common system facilitating the recognition of general regularities.

We hope that the elaborated new method, the detailed experimental analysis will contribute to the better understanding of the wood surface roughness. The material presented is also designed for education purposes, especially for postgraduate students and engineers who completed their studies earlier.

1. Parameters of surface roughness

Machined surfaces always show irregularities of different height and depth; this is what we call *roughness*.
Typical surface roughness profiles for soft and hardwood species are shown in Fig. 1. The first curve demonstrates the surface roughness of Scotch pine of slow growth, where both high and deep irregularities are of small size. The fourth curve illustrates the machined surface of black locust with large vessels, where the height of irregularities are below 10μ but the large vessels cause depth irregularities of size between 50-80 μm.

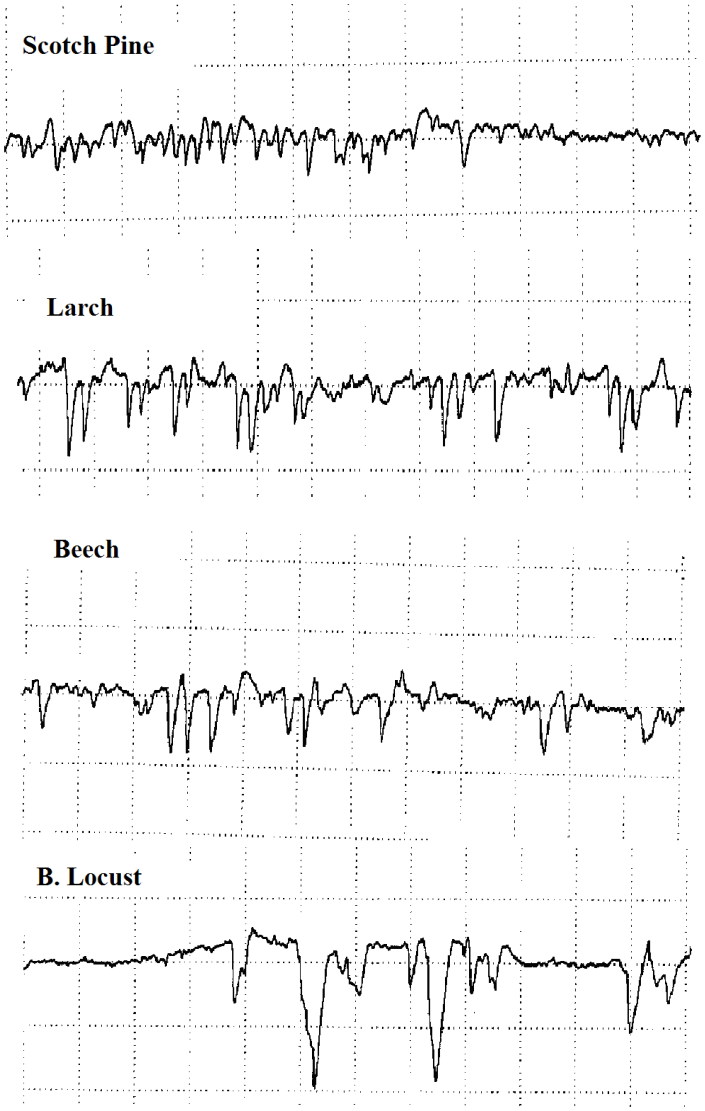

Fig. 1 Surface roughness profiles

It is impossible to find a roughness parameter, which gives an unambiguous characterization of the surface from all aspects; therefore several parameters have been derived, which have been standardized for the purpose of consistent interpretation and usage. (Fig. 2)

R_z	Height of profile elements DIN EN ISO 4287	$R_z = \frac{1}{5} \cdot (Z_1 + Z_2 + Z_3 + Z_4 + Z_5)$ 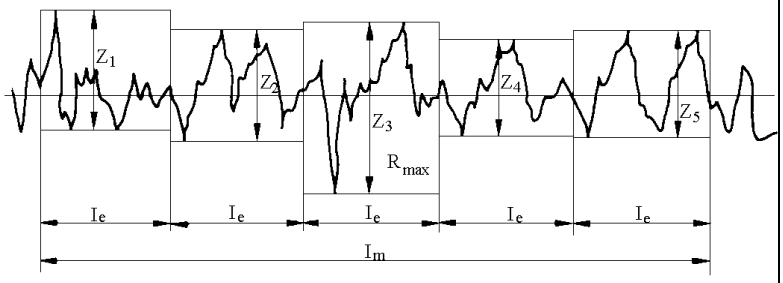
R_{max}	Maximum roughness profile depth DIN EN ISO 4287	
R_a	Average roughness DIN EN ISO 4287	$R_a = \frac{1}{l_m} \int_0^{l_m} \lvert z(x) \rvert \cdot dx$ 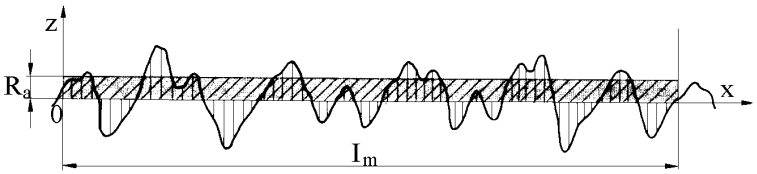
R_{zi}	Profile depth DIN EN ISO 4287	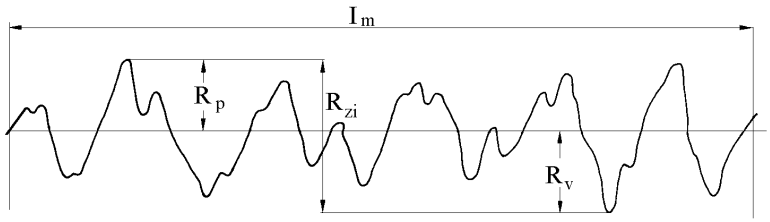
R_p	Roughness profile peak height DIN EN ISO 4287	
R_v	Roughness profile valley depth DIN EN ISO 4287	
W_t	Wave depth DIN EN ISO 4287	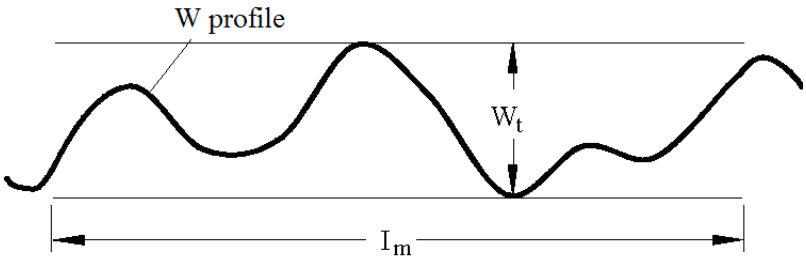

Fig. 2 Standardized parameters of surface roughness and waviness

The truly unfiltered profile also contains accidental waviness on the surface. The surface roughness depth P_z can be applied also for this profile, which has a theoretical correlation to the R_z value of the filtered profile as follows:

$$P_z = R_z + W$$

or

$$\frac{P_z}{R_z} = 1 + \frac{W}{R_z} \tag{1}$$

In practice maximum roughness profile heights do not necessarily fall on peak heights or valley depths, therefore the angle of inclination of the straight line described by the equation (1) will be accordingly smaller; that is:

$$P_z / R_z = 1 + \alpha W / R_z$$

where the value α is less than 1 (generally 0.6-0.8). The range of the measurement values is shown in Fig. 3 [11].

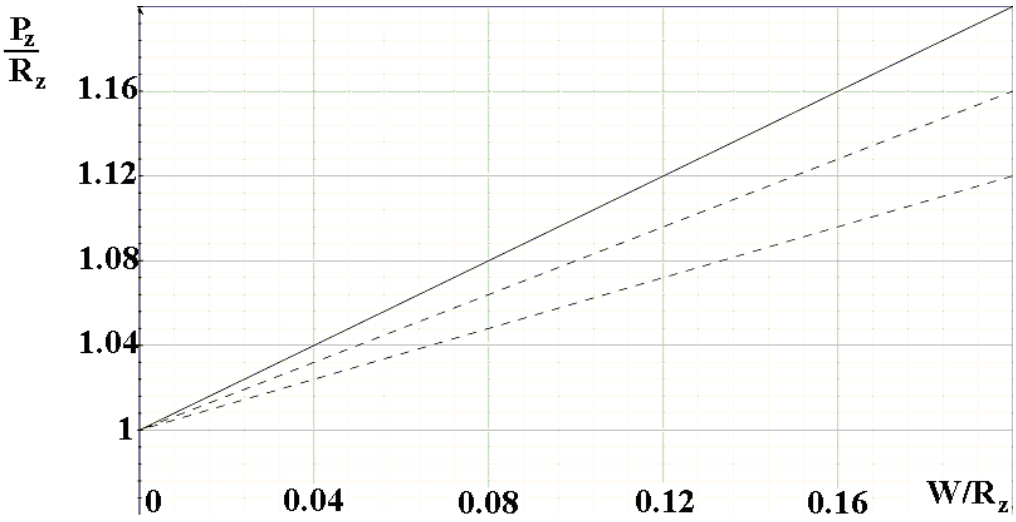

Fig. 3 Roughness of the unfiltered profile in relation to waviness based on the equation (1)
continuous line: theoretical correlation; area between dashed lines: range of the measured values

A part of the space within the roughness profile is filled with material; the rest of the space is filled with air. The relationship between these two factors is expressed by the material ratio curve of the profile (*Abbott curve*) – like in the case of distribution curves. The material ratio curve of the profile is also known as the Abbott curve; its definition method and parameters are shown in Fig. 4. Modern instruments perform this assessment automatically; the data are drawn and can be printed.

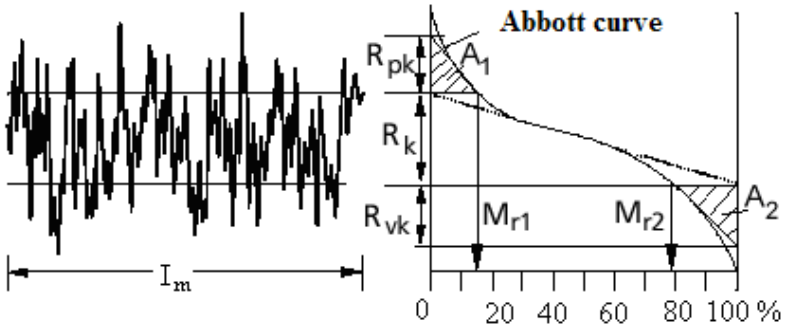

Fig. 4 Calculation and characterization of the material ratio curve (Abbott curve) DIN 4776; DIN EN ISO 4287

R_k - depth of the so-called 'core'
R_{pk} - reduced peak heights
R_{vk} - reduced valley depths
A_1 - material ratio of peak elements
A_2 - surface of valleys
M_{r1} - 'smaller' material portion value of the core
M_{r2} - 'higher' material portion value of the core

2. The anatomical structure of wood

One of the typical characteristic features of wood is the anatomical structure, which has cavities in the form of vessels and cell lumens inside. The typical internal structure of soft and hardwood species is shown in Fig. 5.

The early wood tracheids of Scotch pine have large cavities (20-40 μm) and thin walls, however cavities in the late wood roughly are half of that size. The structure of hardwood species is more complicated, they consist of a number of different cell types. Vessels consisting of vertical units doing the transportation, the diameter size of which can be up to 300 μm; thus they are visible to the eye. The tracheids – cavities in the long parenchyma cells – are relatively small here; they mostly fall in the range 10-20 μm (see Table 1)

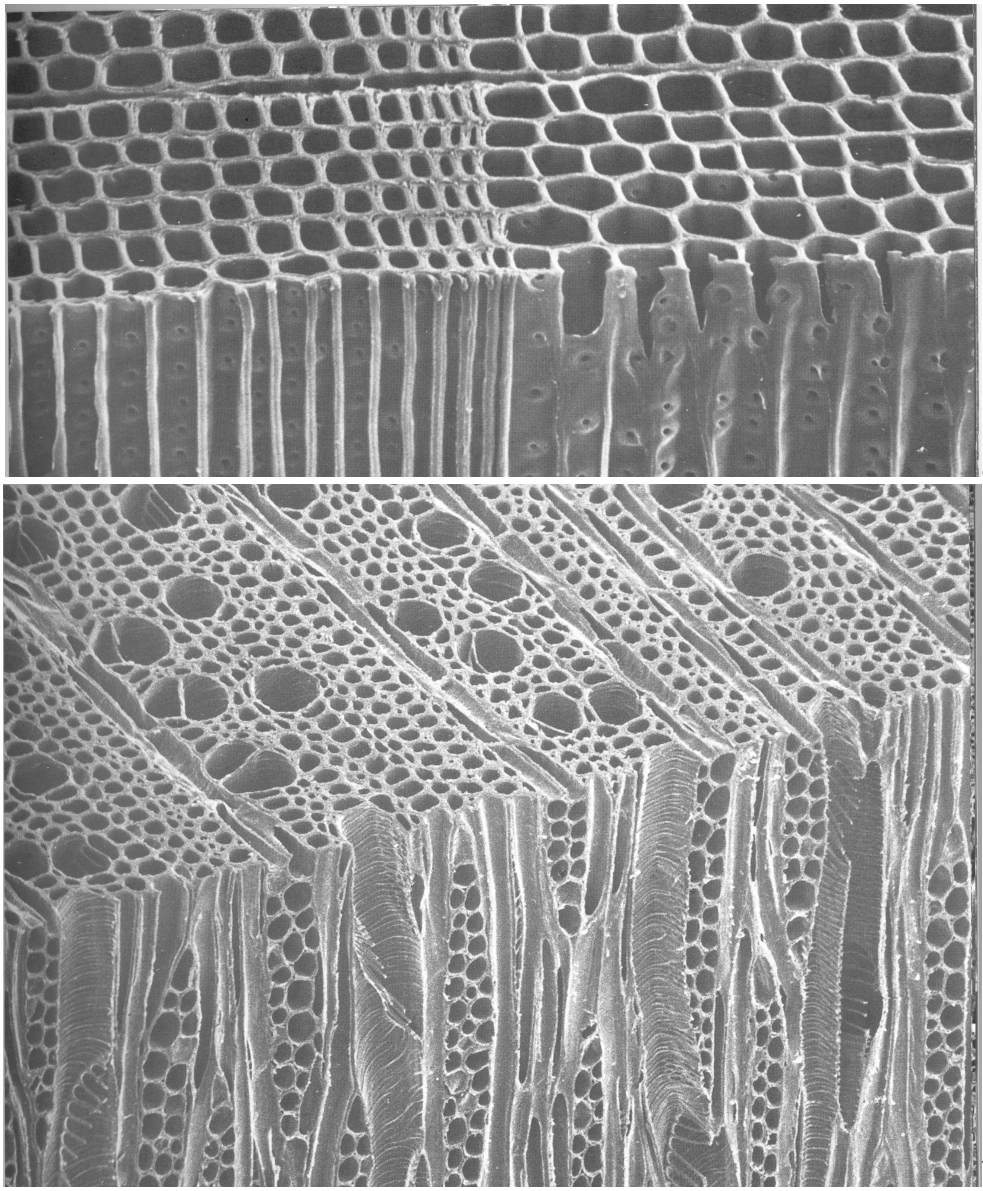

Fig. 5 Microscopic photo of pine (a) and hardwood (b) species

The cavities of both in the vessels and fibres in the early and late wood are also different in size. Furthermore – depending on the weather circumstances – this variability is typical for the internal structure of subsequent annual rings. During mechanical processing of wood cavities are cut in different angles, therefore even in the case of damage-free cutting (sharp cutting line) hollows do remain on the surface. These valleys cause a certain roughness on the surface, which is not effected by the machining process. Therefore the roughness evolving this way is called *structural* or *structure-caused roughness.*

From the roughness aspect, the internal structure of wood is characterized by the mean diameter of cavities and the number of cavities in the particular cross-section unit. The size and number of cavities has to be determined both in the early and late wood, therefore, the early and late wood ratio must also be established.

In order to gain the above data, small-sized sections are taken from different wood species, where the required data are established using a measuring microscope or by means of digital image processing. It is practical to check the obtained data also by calculation methods. The

bulk density of the sample is easy to determine; the following approximation equation has to be effective (based on a 1 cm^3):

$$\rho_t = \left[\left(1 - \frac{d_1^2 \cdot \pi}{4} \cdot n_1 \right) \cdot a + \left(1 - \frac{d_2^2 \cdot \pi}{4} \cdot n_2 \right) \cdot b \right] \cdot \rho \qquad (2)$$

where ρ_t, ρ - bulk density and real density of wood, respectively
d_1, d_2 - mean diameter of cavities in the early and late wood
n_1, n_2 - number of cavities on the unit surface in the early and late wood
a, b - early and late wood portion *(a+b=1).*

We can use the above equation also to double-check the early and the late wood separately, based on the knowledge that the bulk density of late wood is approximately two times higher than that of early wood.

Table1. summarizes the typical characteristics of the anatomical structure of conifer and hardwood species tested.

Table1. Structural properties of specimens

wood species	early wood			late wood		
	$\overline{d_i}$ [μm]	$\overline{n_i}$ [piece/cm^2]	$\bar{a}$	$\overline{d_i}$ [μm]	$\overline{n_i}$ [piece/cm^2]	$\bar{b}$
Thuja	26.5	142 800	0.8482	14.0	316 600	0.1518
spruce	30.0	111 335	0.8478	19.0	160 400	0.1522
pine	28.0	125 100	0.6694	20.0	135 840	0.3306
larch	38.0	65 490	0.6310	17.5	145 000	0.3690
beech (vessel)	66.0	15 740	0.7000	48.0	14 020	0.3000
beech (tracheid)	8.2	342 890		6.4	490 290	
oak (vessel)	260.0	400	0.5900	35.7	12 000	0.4100
oak (tracheid)	22.5	120 000		19.6	85 000	
b. locust (vessel)	230.0	546	0.5800	120.4	1 500	0.4200
b. locust (tracheid)	15.0	270 000		9.6	280 000	
cottonwood (vessel)	69.7	9 500	0.6666	44.0	12 700	0.3333
cottonwood (tracheid)	12.7	309 500		11.0	300 892	
ash (vessel)	177.0	670	0.6100	52.00	750	0.3900
ash (tracheid)	19.0	190 000		14.0	230 000	

Cutting vessels, tracheids and other elements of the texture causes surface irregularities. An important basic data is gained by quantifying the number of vessels cut on a certain length in the direction of machining. The scattering of the vessel diameters usually shows normal distribution, which enables the utilization of the mean diameter size without making a greater error.

The position of the vessels measured to the surface is always accidental, which obviously causes a scattering of the surface roughness obtained.

Adding up the number of structure elements cut on the surface gives a characteristic measure of surface roughness as shown in the model in Fig. 6.
The area of the valleys has a connection with the number and diameter of structure elements measured on a given unit of length in the machining direction, which is expressed in the following equation:

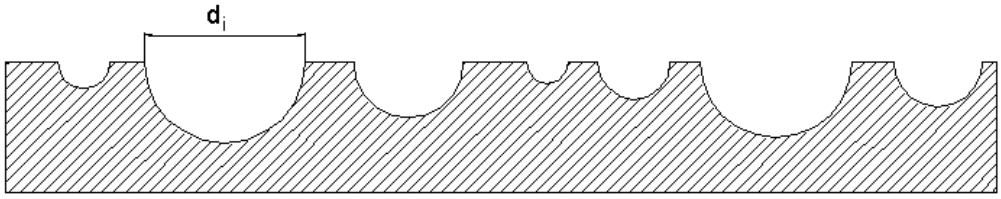

Fig. 6 The model of structural surface roughness

$$\Delta F = \frac{\pi}{8}\left[a \cdot \left(\sqrt{n_1} \cdot d_1^2 + \sqrt{n_2} \cdot d_2^2\right) + b \cdot \left(\sqrt{n_3} \cdot d_3^2 + \sqrt{n_4} \cdot d_4^2\right)\right] \qquad [\mathrm{cm}^2/\mathrm{cm}] \qquad (3)$$

where n_1, n_2 -the number of vessels and tracheids in the early wood in the unit cross-section
n_3, n_4 -the number of vessels and tracheids in the late wood in the unit cross-section
d_1-d_4 -the diameter size of vessels and tracheids in the early and late wood, respectively
a, b -portions of early and late wood

The value ΔF defined with the equation (3) is called *structure number*, which gives an accurate definition of each wood species based on the size and specific number of cavities in the wood structure. Accordingly, surface irregularities caused by the internal wood structure are expected to have a definite correlation with the structure number.
A further advantage of the structure number is that it enables the characterisation of wood species based on their internal structure, and it helps to establish correlations among the surface roughness parameters.
It is well-known that results of surface roughness tests usually show significant scatterings. One of the reasons for this is the accidental position of tracheids and vessels to the machined surface. A further significant scattering can be caused by the accidental position and cut of the early and late wood or the seasonal change of the early wood / late wood ratio, respectively. Namely the value ΔF may have substantial differences in the early and late wood. Pine species show the smallest diviation, whereas hard wood species generate a significantly bigger one. Fig. 7 illustrates the alteration of the ΔF value of different wood species

depending on the early wood ratio. The starting point of the curves (a=0) indicates the pure late wood, while the end point (a=1) indicates the pure early wood. Oak shows the biggest change, but ash also shows a significant one as well.

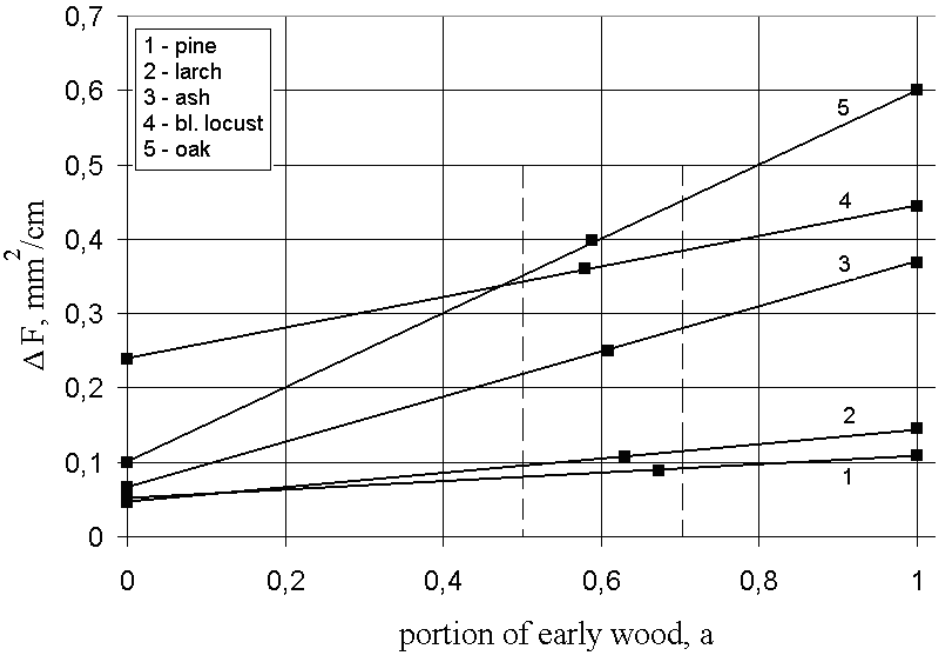

Fig. 7 Alteration of the ΔF value of different wood species in relation to the early wood ratio

Tests show that the early wood ratio falls predominantly in the range a=0.5-0.7 as shown in Fig. 7.

Therefore it seemed practical to apply the relative changes of ΔF for the range a=0.5-0.7 in accordance with the following equation:

$$\delta(\Delta F) = \frac{\Delta F_{0.7} - \Delta F_{0.5}}{\Delta F_{0.6}} \tag{4}$$

Wood species can be characterized with the ratio of cross sections of cavities cut in the early and late wood, which we can express using equation (3) as follows:

$$B = \frac{d_1^2 \cdot \sqrt{n_1} + d_2^2 \cdot \sqrt{n_2}}{d_3^2 \cdot \sqrt{n_3} + d_4^2 \cdot \sqrt{n_4}} \tag{5}$$

Since pine species have the vessels missing, thus the equation (5) for conifers will be more simple.

Fig. 8 shows the relative changes of ΔF in relation to the parameter B defined with equation (5).

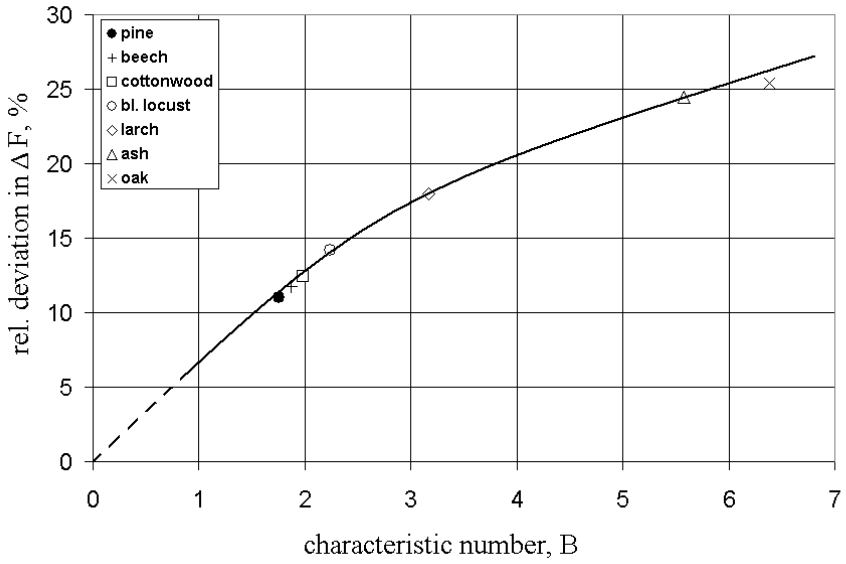

Fig. 8 Relative changes of ΔF in relation to the parameter B

The apparent correlation between the two variables is displayed clearly. However it is remarkable that beech is located right next to Scotch pine; whilst black locust shows a smaller relative change than larch. Consequently the relative change has no connection with the absolute value of ΔF. The correlation obeys on the following empiric equation:

$$\delta(\Delta F) = 7.8 \cdot B^{0.65} \quad [\%] \tag{6}$$

3. The origin of surface roughness

Roughness that evolves during machining has two major components: machining-caused roughness and roughness caused by the anatomical wood structure. Even in the case of an ideal machining rough surface evolves due to the inner cavities cut. Moreover in the recent practice of high-speed machining, roughness due to machining is usually much less than the structure-based roughness, especially in the case of hardwood species with large vessels.
The roughness due to machining usually depends on the following factors: cutting speed, chip thickness, cutting direction relatively to the grain, rake angle of the tool, sharpness of the tool edge (tool edge radius) and vibration amplitude of the work piece.
Wood cutting belongs to the group of the so-called free cutting. Its main characteristic feature is the absence of a counter-edge, therefore, the counterforce is produced by the strength of wood and forces of inertia. The higher the strength and hardness parameters (modulus E) the wood has the smaller force of inertia is required; that means, the slower the roughness increases with the decrease of the cutting speed.

The primary reason for machining-caused roughness is the brittle fracture of the material and its low tensile strength perpendicular to the grain. The occurrence of brittle fracture cannot be

eliminated, however, it can be limited to a lower volume. The most effective method for this is the high-speed cutting and the smallest material contact possible (sharp tool edge).

The only way to eliminate the negative effect of the low tensile strength perpendicular to the grain is to generate a compression load in the immediate vicinity of the edge. This can be facilitated with a 65-70° tool angle or a 20-25° rake angle. Especially the edge machining of boards is very inclined to breaking the edge because of the tensile load; therefore the selection of appropriate kinematic conditions is very important [10].

An excessive compression load deforming the material can also cause roughness. The method 'smooth machining' has been known for a long time, which is based on the knowledge that smaller chip thickness raises smaller forces. Compression load can also be reduced by using the 'slide cutting'. Slide cutting produces shear load on the edge, which also contributes to material failure. In accordance with the well-known equation the equivalent stress has the following form [12]:

$$\sigma_e = \sqrt{\sigma^2 + 4\tau^2} \ .$$

The distribution of compression load inside the material depends on the tool edge radius (bluntness of the tool edge). Due to the thickness of the edge a layer in the material of thickness z_0 will be compressed underneath the edge (Fig. 9).

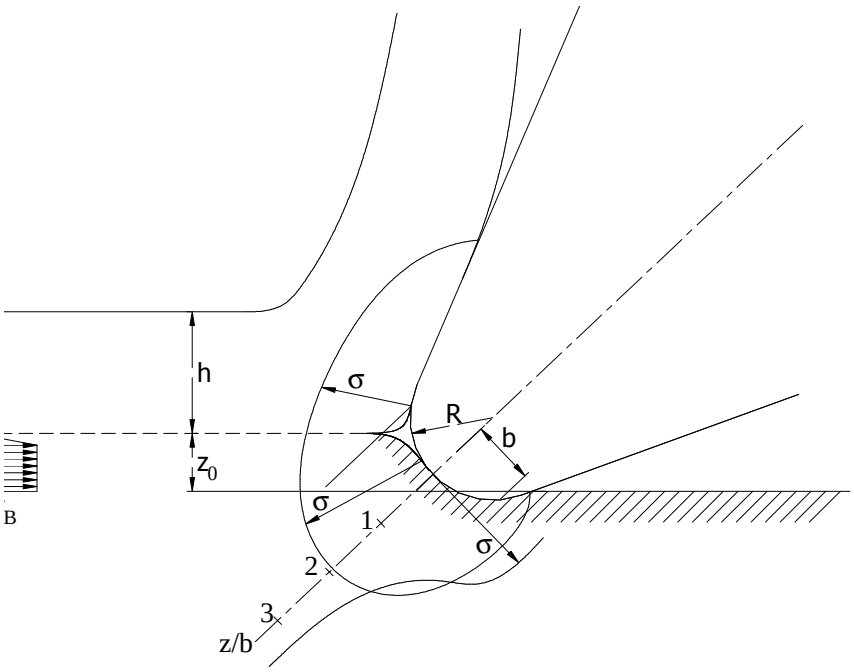

Fig. 9 Compression effect of the edge

This layers thickness is about 70% of the tool edge radius. The load of the edge will be transferred onto the material on a surface with a *2b* width and a length that is identical with that of the edge. This is similar to the strip load. The biggest load appears just under the

contact surface and it rapidly decreases as we move towards the inside of the material. This means that the highest compression of cells always starts directly underneath the edge.

If the compression load underneath the edge reaches the ultimate bearing stress of the material the cell system suffers permanent deformation and it gets compressed to the detriment of the cavities [1]. If out of total deformation z_0 the permanent deformation is z_1, then the expelled material will be located in the lower layers and the thickness of the compressed layer z_2 is accordingly (see Fig. 31):

$$z_2 = z_1 \cdot \rho_1 / (\rho_2 - \rho_1) \tag{7}$$

where ρ_1 – is the volume density without compression
ρ_2 – is the volume density of the compressed material (1-1.2 g/cm^3)

The volume density of early and late wood is significantly different, while the value ρ_2 can change only to a limited extent; therefore we can expect the following values after compression: approximately $z_2=z_1$ in the early wood and $z_2 \cong 3z_1$ in the late wood.

The deformation underneath the edge is elastic in the first period of the compression; it will therefore rebound once the edge has passed by. The approximate rate of elastic deformation can be calculated easily. When the elastic half space is exposed to a strip load:

$$\sigma = \frac{E}{2 \cdot \left(1 - \nu^2\right)} \cdot \frac{z}{2b} \tag{8}$$

If for the purpose of simplicity we presume that the elastic deformation z_r is sustained till the crushing stress σ_B is reached, then:

$$z_r = \frac{\sigma_B 4b\left(1 - \nu^2\right)}{E} \tag{9}$$

In the case of pinewood compression load between the directions B and C can have values σ_B=15 N/mm^2, then a R=10 μm radius is likely to produce elastic deformation of approximately z_r=1 μm, while a R=50 μm radius is expected to bring elastic deformation of approximately z_r=5 μm. These values give one seventh of the total deformation expected (z_0=7 μm and 35 μm, respectively). The above results would have the logical consequence that the compression of the upper layer with permanent deformation should be considered in each case.

The wood structure however contains cavities; and even cavities of smaller size can be measured to the radius of a sharp tool edge. Therefore the sharp tool edge can penetrate the cavities and break the cell walls. The tool edge bends these broken wood parts standing

vertically, which then take the necessary deformation z_0 without transferring it towards the lower layers. When the tool edge radius is increased, both the edge size and the rate of deformation z_0 exceed the size of cavities; consequently a compression of the surface layer evolves. An approximately R=20 μm tool edge radius is expected to trigger a surface compression with permanent deformation.

4. Measuring instruments and methods

The common measurement methods are summarized in Table 2.

Table 2.

Measurement methods	**Destructive**	**Contact**	**Non-contact**	
			Optical	**Non-optical**
With profile display	Raster microscopy based on the tunnel effect	Mechanical stylus instruments (Perthometer)	Laser pick-up instruments - laser focusing method - triangulation method	
Without profile display	Flemming gel spread test			Capacity method Pneumatic method

Among the methods listed above mechanical stylus instruments – the so-called perthometers – are applied mainly. Furthermore optical laser pick-up instruments (laser focusing method and triangulation method) are subjects of ongoing experimentations.

Mechanical stylus instruments cut a two-dimension profile from the actually three-dimension surface. It is obvious that 'covered' cavities cannot be determined by means of stylus instruments. The stylus has always definite geometrical dimensions (stylus edge radius, cone angle). These mechanical dimensions perform a so-called mechanical filtering.

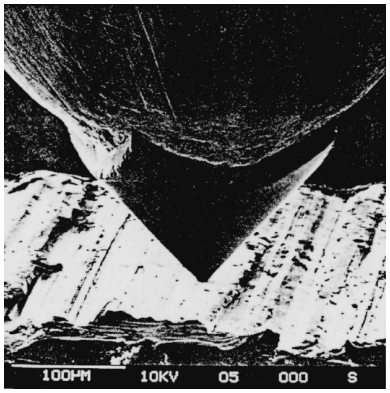

Fig. 10 Diamond stylus tip on a metal surface in high magnification

The pressing force of the stylus has decreased to a value around 0.8-7 mN by today, thus it has no detrimental effects on the surface. During testing on a Scotch pine probe no surface damage was experienced at a 40-times repetition. [13]. However, there is a special case when even this minimal pressing force could become problematic: if the stylus contacts a free fibre – that is still connected to the surface at its other end – in a perpendicular direction. In this case the stylus simply pushes the fibre aside. The same phenomenon brings an advantageous effect when the stylus meets a particle of dust on the surface. The working principle of perthometers is shown in Fig. 12:

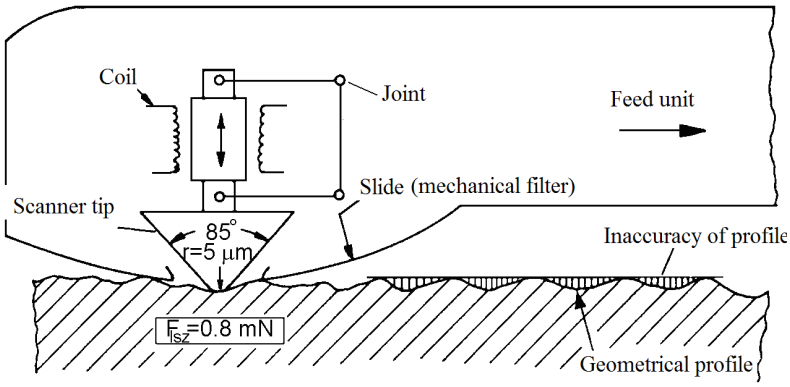

Fig. 11 Installation of the stylus

The diamond stylus tip is installed with a suspension of minimal friction resistance. While the stylus is drawn at a constant speed, an electromechanical converter (differential transformer) converts the vertical shift of the stylus into an electric voltage (see Fig. 11).

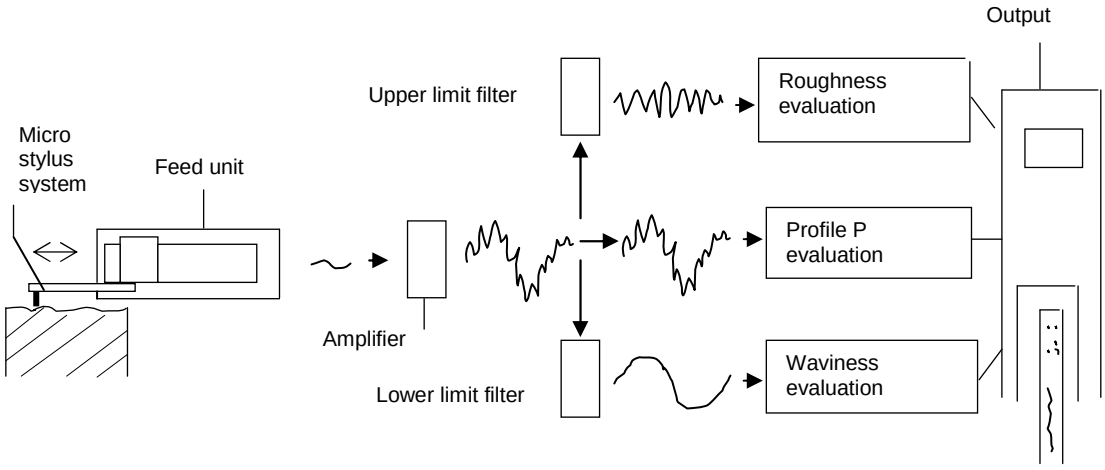

Fig. 12 The working principle of perthometers

The signal is first amplified and then evaluated (Fig. 12). For the purpose of evaluation, roughness is separated from waviness by means of frequency filtering. A detailed discussion of frequency filtering will follow later on. Some manufacturers enable the installation not only of a mechanical micro stylus system on the feed but also that of an optical micro stylus system; for instance the instrument 'Focodyn' by Mahr (which uses the laser focusing principle).

Feed unit installation patterns are shown in Fig. 13.

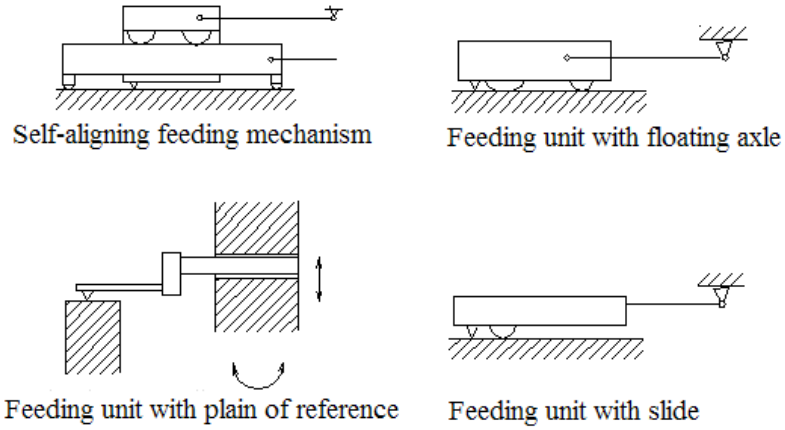

Fig. 13 Feed unit installation patterns

The most common type of feed unit is the third one – a feed unit with a reference surface, which however requires equalization prior to measuring.

Laser pick-up methods also cut a two-dimension profile from the surface, however without establishing a mechanical connection. Figs 14 and 15 show the measuring principle of the two most common types of laser pick-up instruments:

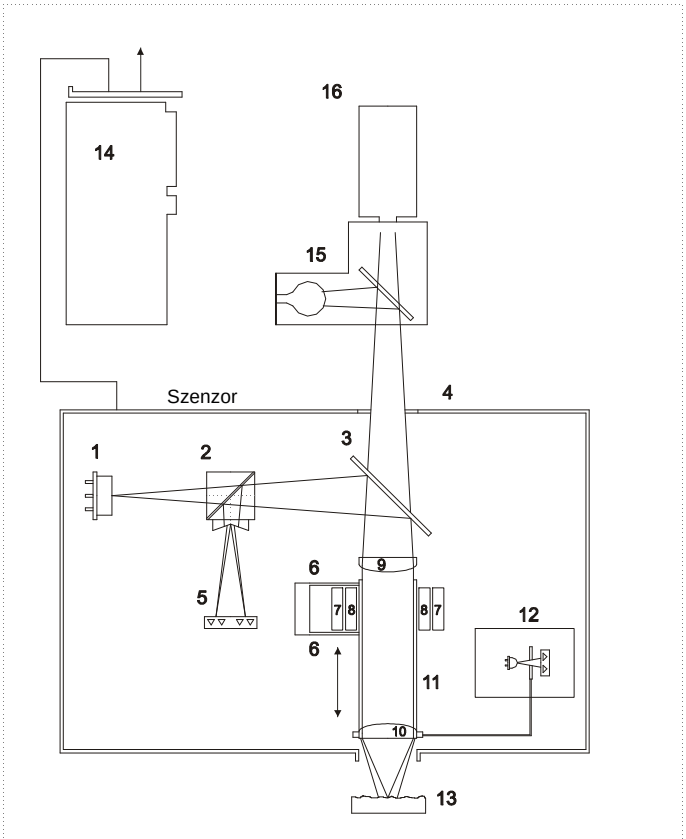

1. Laser diode
2. Prism with division mirror
3. Division mirror
4. Gauge
5. Photo diode
6. Flat springs
7. Coil
8. Magnet
9. Collimator lens
10. Objective
11. Tube
12. Photocell measuring system
13. Surface measured
14. PC-card
15. Microscope + illumination
16. OCD camera

Fig. 14 The laser focusing method

The laser focus instrument focuses the beam from a laser diode on the surface, which means that the respective objective setting always provides a sharp image. The instrument registers the vertical shift that the objective makes in order to set the image sharp; this record is then evaluated.

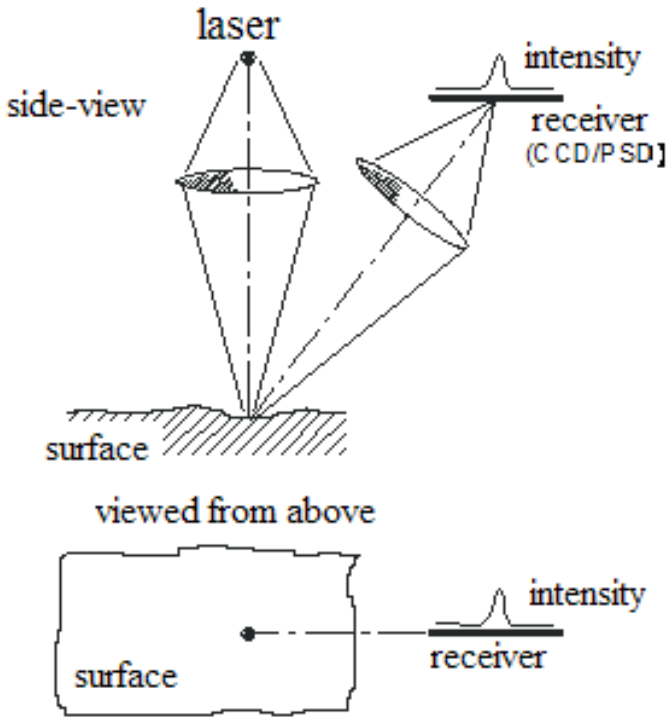

Fig. 15 The triangulation method

In the case of the triangulation method the instrument targets the laser beam towards the surface, following which the beam is focused on the surface by an optical system. A decoder determines the intensity rate of the reflected beam, which depends on the surface structure. The intensity rate then stands for the measure signal, based on which the surface profile can be plotted. This measurement system has the advantage that it can be applied not only perpendicularly to the surface but also at deviations of small degrees. Nevertheless a significant disadvantage is that the measurement is influenced by the colour and tone differences of the surface measured. Colour and tone differences are often registered as a height difference. (It is very unfavourable when wood is measured: e.g. colour differences in the early and late wood).

Wood is always measured perpendicularly to the grain. The following optional sampling lengths can be set for the stylus: 0.56, 1.75, 5.5, 17.5 and 56 mm. It is practical to measure as many annual rings as possible; accordingly the longer feeds should be selected for textures with wider annual rings.

5. The effects of machining process on surface roughness

It is well known that a higher cutting speed results in a smoother surface; this means that smaller roughness values are achieved in terms of both the average surface roughness R_a, and depth of irregularities R_z. Expanding the assessment also on the characteristics of the *Abbott curve* we receive the following results (Figs 16 and 17):

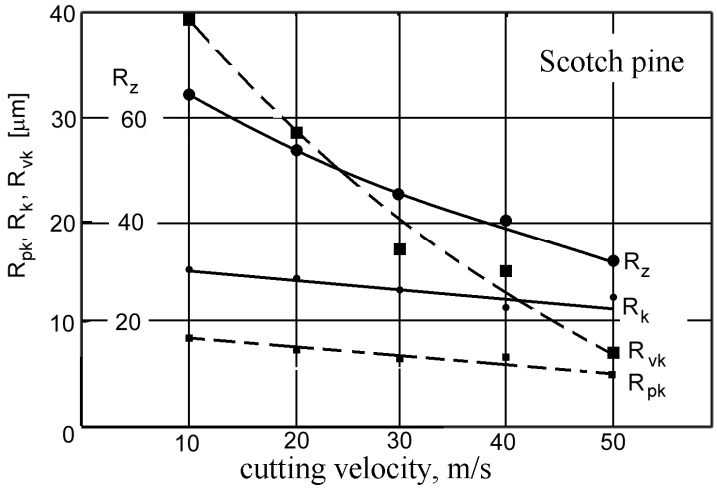

Fig. 16 Effects of cutting speed on the surface roughness parameters for Scotch pine

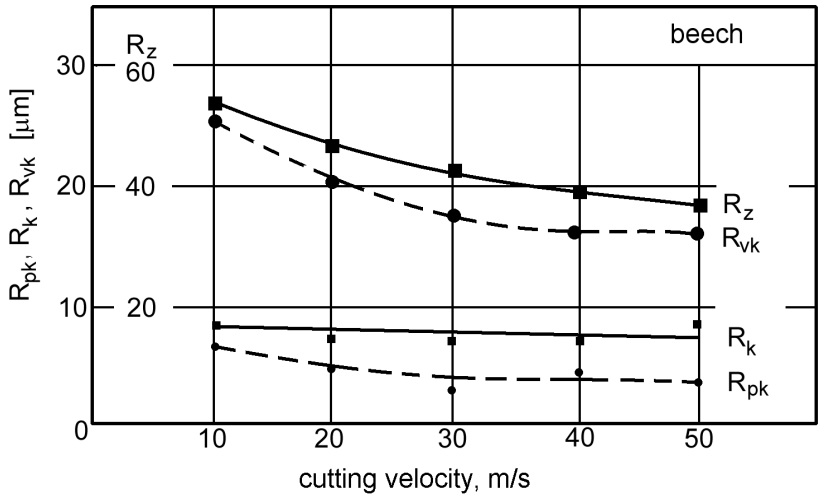

Fig. 17 Effects of cutting speed on the surface roughness parameters for beechwood

In the case of beech the average diameter of vessels was 60 µm, while for tracheids the corresponding value was 10-15 µm. In the case of Scotch pine the mean inner diameter of the tracheids was 25-30 µm in the early wood and 13-18 µm in the late wood.

From Fig. 16 and Fig. 17 it can be concluded that in both cases the R_{pk} and R_k values remain nearly constant or slightly decrease as a function of cutting speed. On the other hand, R_{vk}-values fundamentally depend on cutting speed. It may also be seen that, in case of pine, this dependence is stronger, especially at low cutting velocities. This result may be explained by the fact that the pine wood had smaller local stiffness around the cutting edge, therefore, inertia forces play a more important role to ensure a clear cutting surface. At the same time, beech had larger structural cavities giving greater R_{vk}-values even at high cutting velocities.

As we concluded previously, chip thickness or feed per tooth also influences the surface roughness to a smaller extent. This is explained by the fact that the increase of the chip thickness also raises increased forces, and the thicker chip can transmit bigger forces on the connected area at the point of chip detachment.

Fig. 18 shows the effect that feed per tooth (e_z) exerts on irregularity depth (R_z)

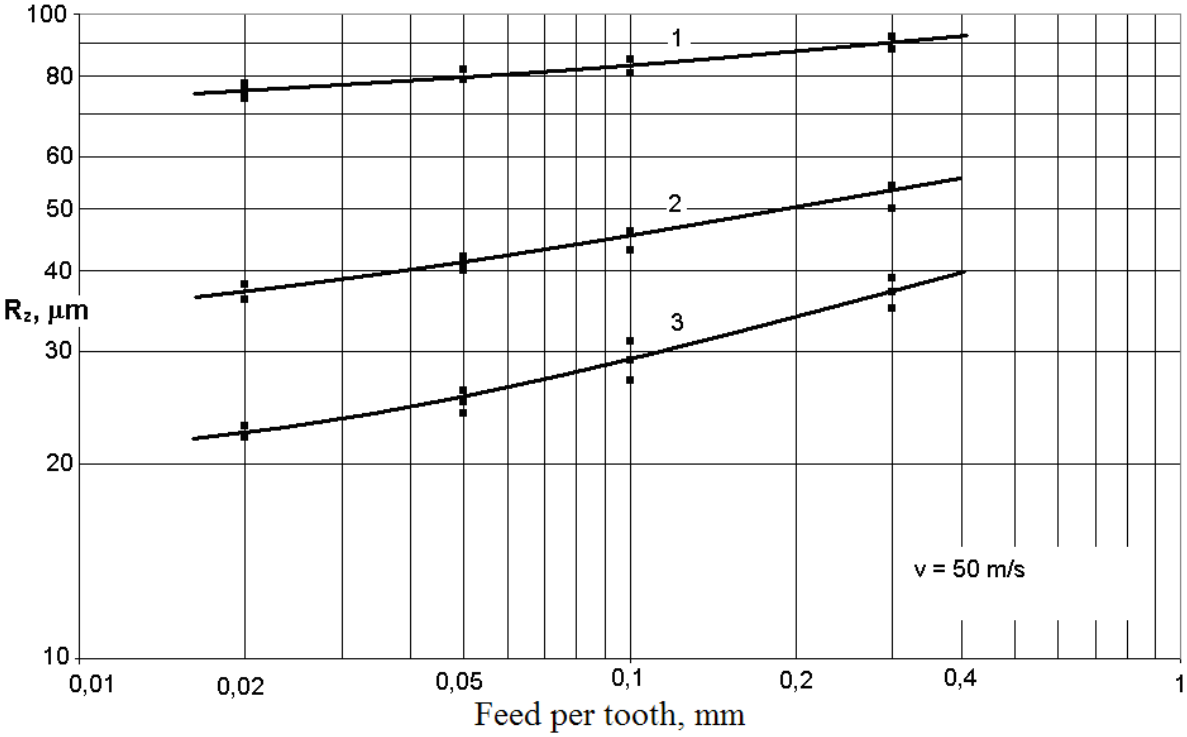

Fig. 18 Effects of feed per tooth (e_z) on irregularity depth (R_z)
1-oak; 2-beech; 3-Scotch pine

The softer the machined wood is the bigger is the effect of feed per tooth. The combined parameter of the *Abbott curve* (R_k+R_{vk}) also shows good correlation with the feed per tooth, as illustrated in Fig. 19.

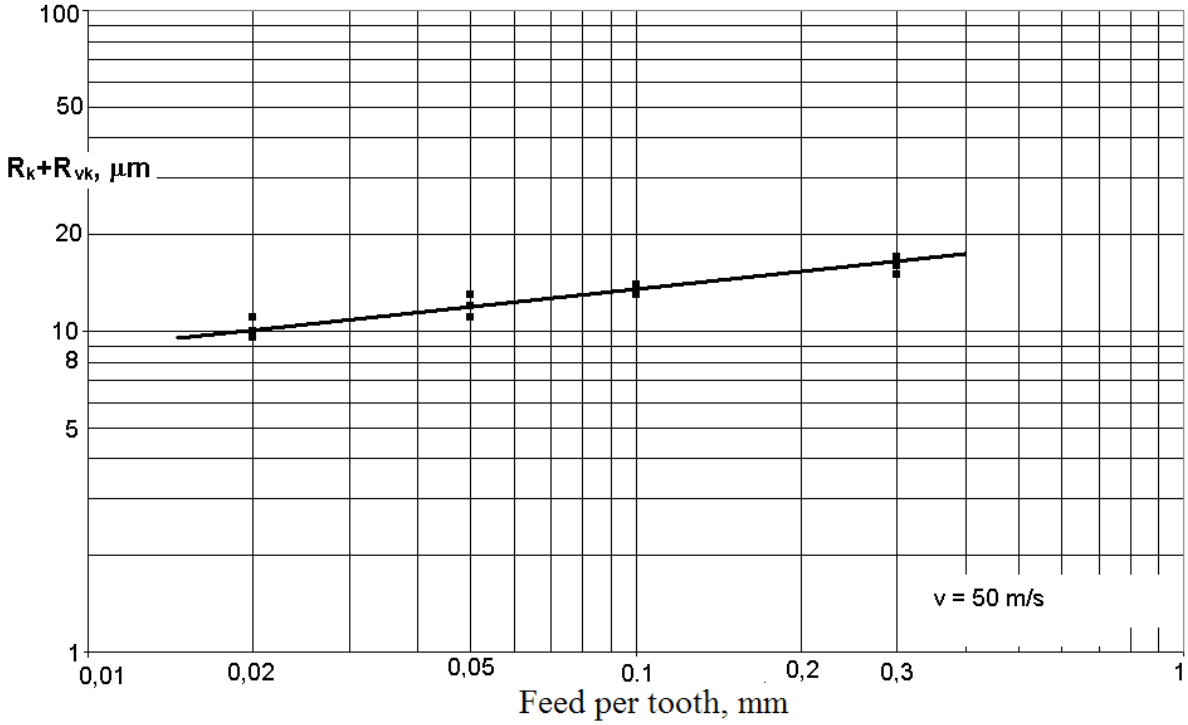

Fig. 19 Effects of feed per tooth e_z on the combined parameter (R_k+R_{vk}) in the case of Scotch pine

Increasing the feed per tooth also increases the reduced valley depth R_{vk}.

The curves in Fig. 18 can also be expressed in the form as follows:

$$R_z = A + B \cdot {e_z}^n \tag{10}$$

where A, B and n are constant values. The value of exponent is 0,6 for all of the three curves, and the value of B is also closely identical.

6. Internal relationships between roughness parameters

Examining the correlations between the common roughness parameters (average roughness R_a, irregularity depth R_z) and the *Abbott curve* we can discover some interesting interrelations(Figs. 20 and 21): Fig. 20 shows a strong relationship between the average roughness and the sum of Abbott parameters.

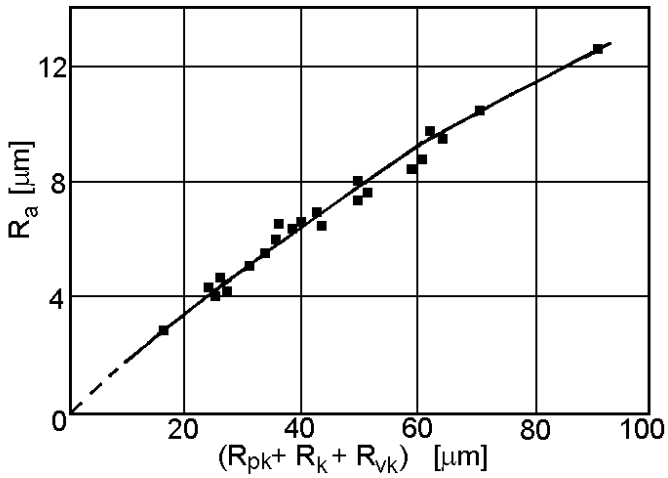

Fig. 20 Relationship between R_a and the *Abbott-parameters*

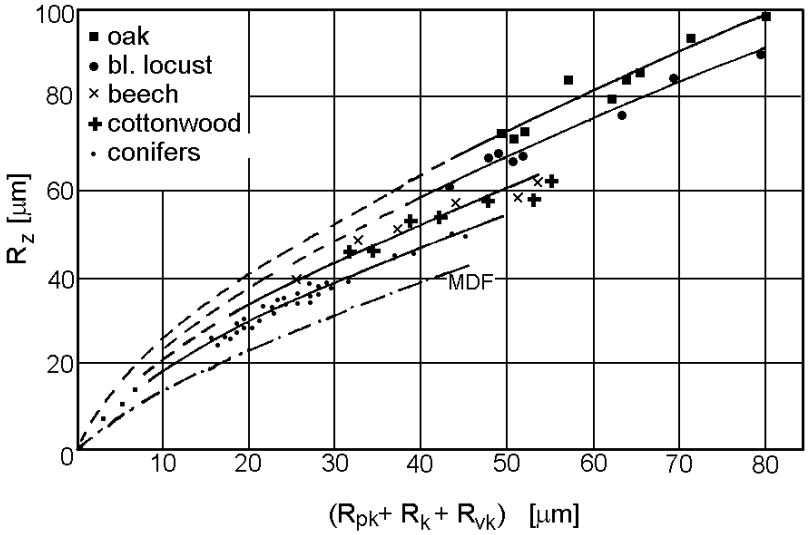

Fig. 21 Relationship between irregularity depth R_z and the *Abbott-parameters*

It is well-known that between R_a and R_z only a poor interrelation exists. As a consequence, no uniquely defined relationship between R_z and the sum of Abbott-parameters can be expected. Nevertheless, the experimental results depicted in Fig.21 show an interesting picture.

A lot of curves are obtained and, as an addition for a more accurate explanation, the measurement results on MDF-boards of different volume density included [7]. MDF has the more uniform internal structure which gives the lowest curve. The oak possesses large vessels and hereby a much less uniform structure and, therefore, gives the uppermost curve. The curves for other species are lying between the two extremes according to their inhomogeneities. The lot of curves obeys the following general form

$$R_z = A \cdot \left(R_{pk} + R_k + R_{vk}\right)^{0.65} \tag{11}$$

and the constant can be expressed as

$$A = 7.45 \cdot \left(R_k + R_{vk}\right) / R_z \tag{12}$$

Using the Abbott curve, the lack of material in the uneven surface can be determined. An equivalent layer thickness may be calculated (see Fig. 4) as follows

$$\Delta h_e = R_{pk} \cdot \left(1 - \frac{M_{r1}}{2}\right) + \frac{R_k}{2} + \frac{R_{vk} \cdot \left(1 - M_{r2}\right)}{2} \tag{13}$$

where M_{r1} and M_{r2} should be substituted as decimal values. The following rough estimation shows the weight of the parts in Eq. (13):

$$\Delta h_e = 0.95 \cdot R_{pk} + 0.5 \cdot R_k + 0.08 \cdot R_{vk} \tag{14}$$

In practical cases the R_{pk}-layer can eventually be neglected due to the fact that the few peaks sticking out from the surface can easily be crushed by pressing.

The graphical representation of the lack of materials related to the unit surface is seen in Fig. 22 The upper curve refers to the case including also the R_{pk}-layer. The scattering of measurement data is somewhat higher than in the case excluding the R_{pk}-layer.

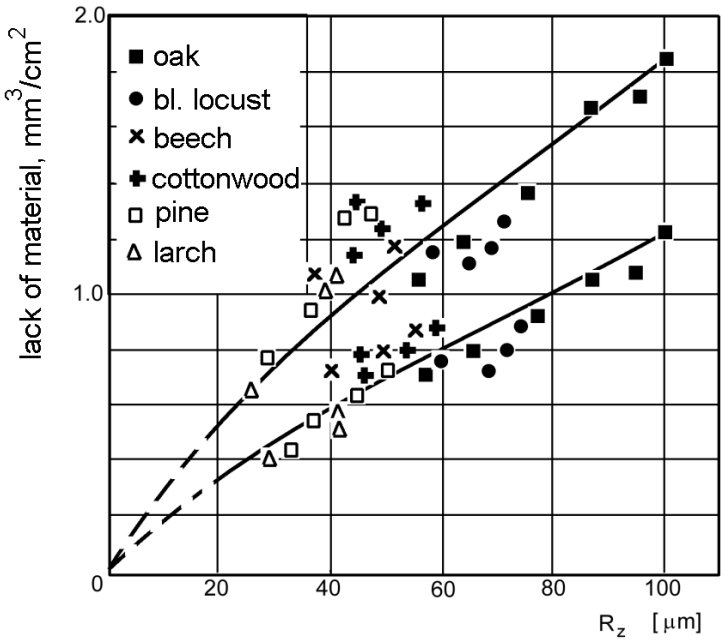

Fig. 22 Relationship between irregularity depth R_z and the lack of material in the surface
1 – R_{pk}-layer is included; 2 – without R_{pk}-layer

7. The use of Structure Number

The determination of the structure number ΔF for wood species has become feasible by using the data of Table 1. and equation (3). The structure number gives an unique characterization of a particular wood species from the internal structure aspect. Furthermore differences caused by the area of growing can be taken into consideration, too. Therefore the structure number is expected to have a definite correlation with the roughness parameters, regardless of the wood species and the area they were grown.

The relationship that was established by evaluating 10 different wood species is shown in Fig. 23.

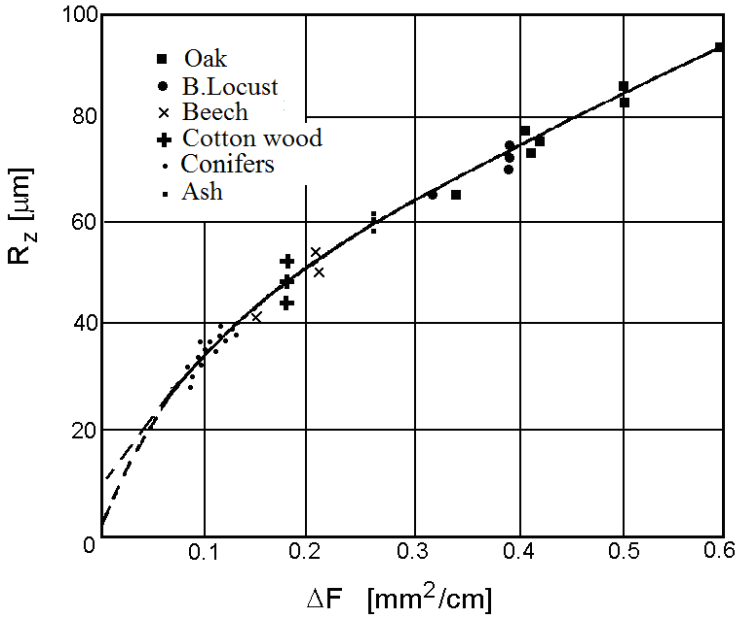

Fig. 23 Relationship between irregularity depth R_z and the structure number ΔF based on the parameters of 10 wood species

This curve demonstrates the best surface roughness that can be achieved in practice as a function of the structure number. The relationship can be described with the following empiric equation:

$$R_z = 122 \cdot \Delta F^{0.55} \tag{15}$$

In order to calculate the structure number, the size and specific number of vessels and tracheids are needed. From each specimen used to roughness measurements additional small specimens were cut to determine the structural properties. While the structure number is sensitive to the accuracy of experimental data, a combined image processing method and light microscope method was used. The image processing method alone generally gave results not accurate enough. The measured data are summarized in Table 1.
In order to separate the roughness components three 20 by 5 cm samples were tangentially cut from each wood species and after machining they were subjected to finishing using a special finishing machine. The finishing was repeated until the measured profile was flat and so suitable for evaluation.

Establishing the finished surfaces, the same samples were subjected to milling operation using various cutting speeds between 10 and 50 m/s. These surfaces were evaluated with the common surface measuring methods.

On the finished surfaces a hypothetical base line was first established and, taking only the positive amplitudes into consideration, the corresponding R_z'-value was calculated (Fig. 24). This is the roughness component due to woodworking operation. Knowing the overall R_z-value and the latter subtracted from it, we get to an R_z-value due to the internal structure of wood.

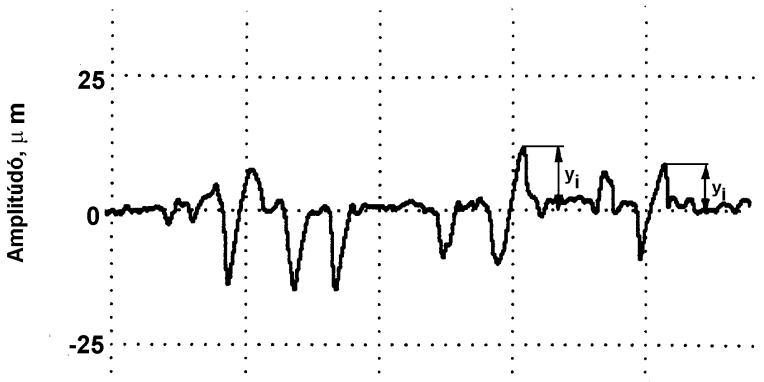

Fig. 24 Measurement of the roughness component due to machining

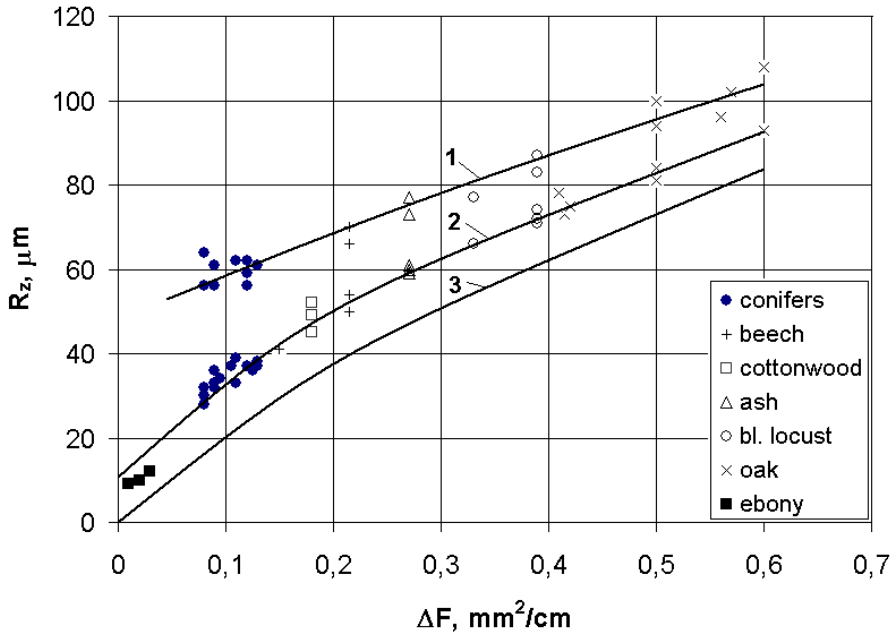

Fig. 25 Irregularity depth R_z, as the best achievable processing roughness in relation to the structure number ΔF
1-cutting speed 10 m/s; 2- cutting speed 50 m/s; 3-anatomical roughness

Calculation of the machining roughness component enables the calculation and plotting of anatomical roughness. The anatomical roughness determined with this method is the smallest roughness that can be achieved on the given sample at all.
Fig. 25 shows the anatomical roughness and the actual roughness as a function of structure number at two different cutting speeds.

A general relationship for Fig. 25 can be expressed in the following empirical form:

$$R_z = \left(123\Delta F^{0,75} + 35e_z^{0,6}\right)\cdot\left(1+\frac{50-v_x}{50}\frac{0{,}1183}{\Delta F^{0,83}}\right) \qquad (16)$$
$$10m/s \le v_x \le 50m/s$$

where ΔF must be substituted in mm^2/cm, e_z in mm, and v_x in m/s. The third part of Eq. (16) as well as the curves illustrate clearly that the softer pine wood is more sensitive to a decrease in cutting speed. This phenomenon can be explained with the smaller local rigidity of pine, which was already mentioned before.
Using a sufficient high cutting speed, it appeared that the surface roughness will rather be determined by the internal structure of wood.
In the following we discuss surface roughness parameter ratios, which show uniquely defined correlations with the structure number ΔF.

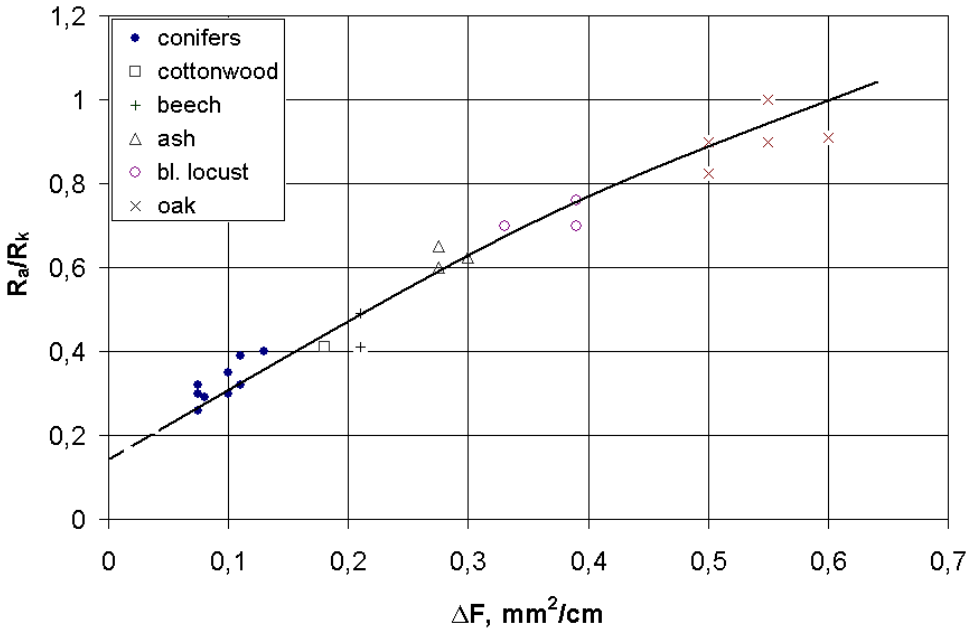

Fig. 26 Correlation between the relationship R_a/R_k and the structure number ΔF

Fig. 26 illustrates the correlation between the relationship R_a/R_k and the structure number ΔF. The anatomical structure of wood causes a fivefold variation in the R_a/R_k ratios. This leads to the conclusion that wood species cannot be compared on the simple basis of surface roughness.

Fig. 27 shows the correlation between the R_{vk}/R_z ratio and the structure number ΔF. Here we have a threefold extent of alteration.

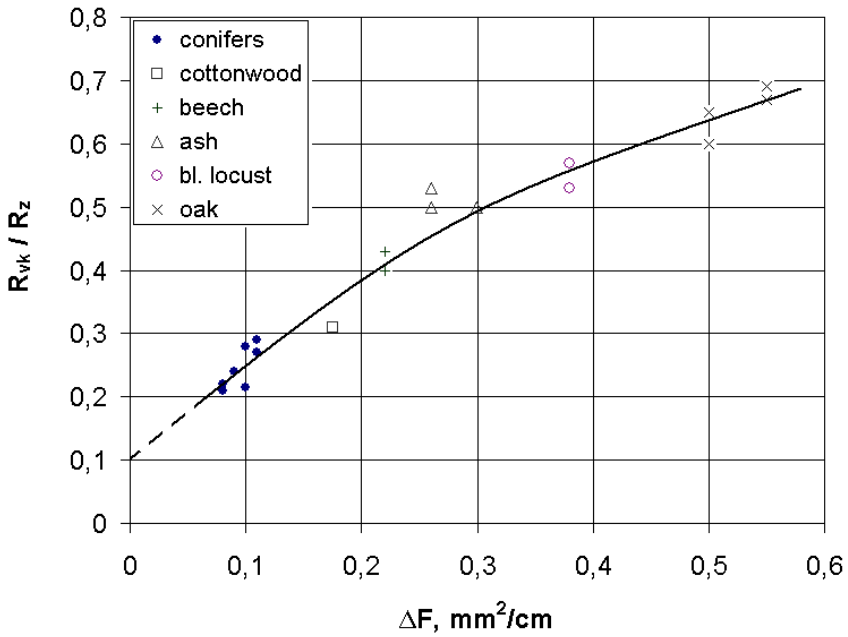

Fig. 27 Correlation between the relationship R_{vk}/R_z and the structure number ΔF

Finally we examined how the core depth of the material ratio curve (R_k) effects the surface roughness as a function of the structure number ΔF.

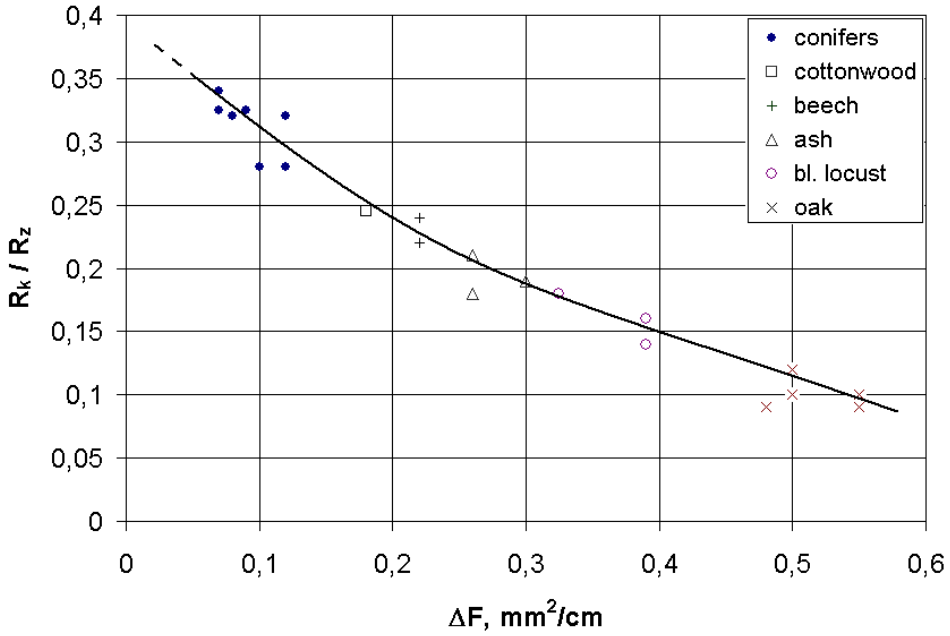

Fig. 28 Correlation between the relationship R_k/R_z and the structure number ΔF

Fig. 28 demonstrates that the value of R_k influences the roughness to a greater extent in the case of soft wood species. It should be noted that the correlation curve in Fig. 28 is valid for sharp tools only. Namely, the value of R_k is dependent on tool sharpness independently of wood species.

8. Effects of tool wear on the surface roughness

It is a well-known fact that enhanced wear of the tool increases the surface roughness. This is the ultimate practical reason why tools are re-edged based on a certain working time or cutting length completed.

Blunt tools with a bigger edge radius transmit bigger forces on the material; the material in front of the tool travels a longer distance going around the edge. The forces transmitted on the chip at the detachment point cause a fracture of elementary particles. Fractures beneath the cutting level are primarily expressed in the Abbott parameter R_k;, therefore this parameter is expected to be highly sensitive to tool edge deterioration.

Fig. 29 shows the alteration of the R_k parameter of four different wood species when using two different tool edge radii.

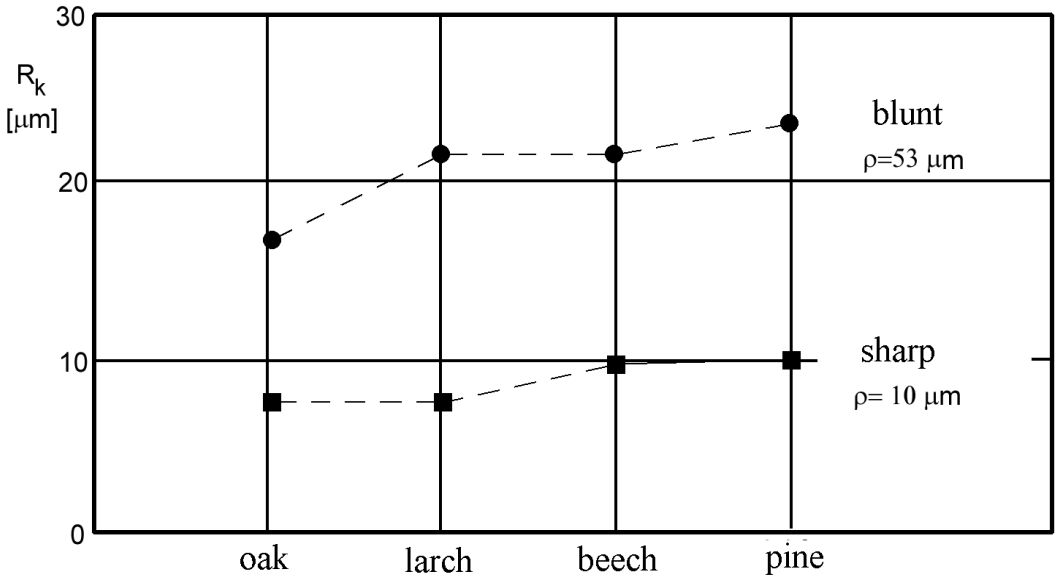

Fig. 29 Alteration of the R_k value when using sharp and blunt tool edges in relation to four different wood species

It is clearly visible that the parameter R_k showed a twofold increase in each case in comparison to cutting with sharp edges. These data lead us to conclude that the parameter R_k gives a good feedback on the deterioration status of the tool edge.

The tool edge radius usually increases the roughness parameter R_z in a linear way. Fig. 30 illustrates the correlation that was established by testing Scotch pine and beech samples.

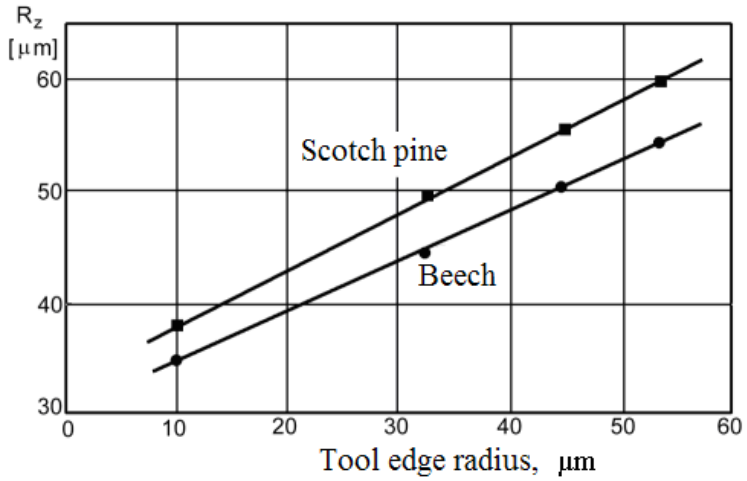

Fig. 30 Correlation between the parameter R_z and the tool edge radius established by testing

We already have mentioned the compressing effect of a blunt tool edge. The compression of the surface can already be observed at an approximately hundredfold microscopic magnification. This phenomenon on a machined Scotch pine probe is shown in Fig. 31. [1]

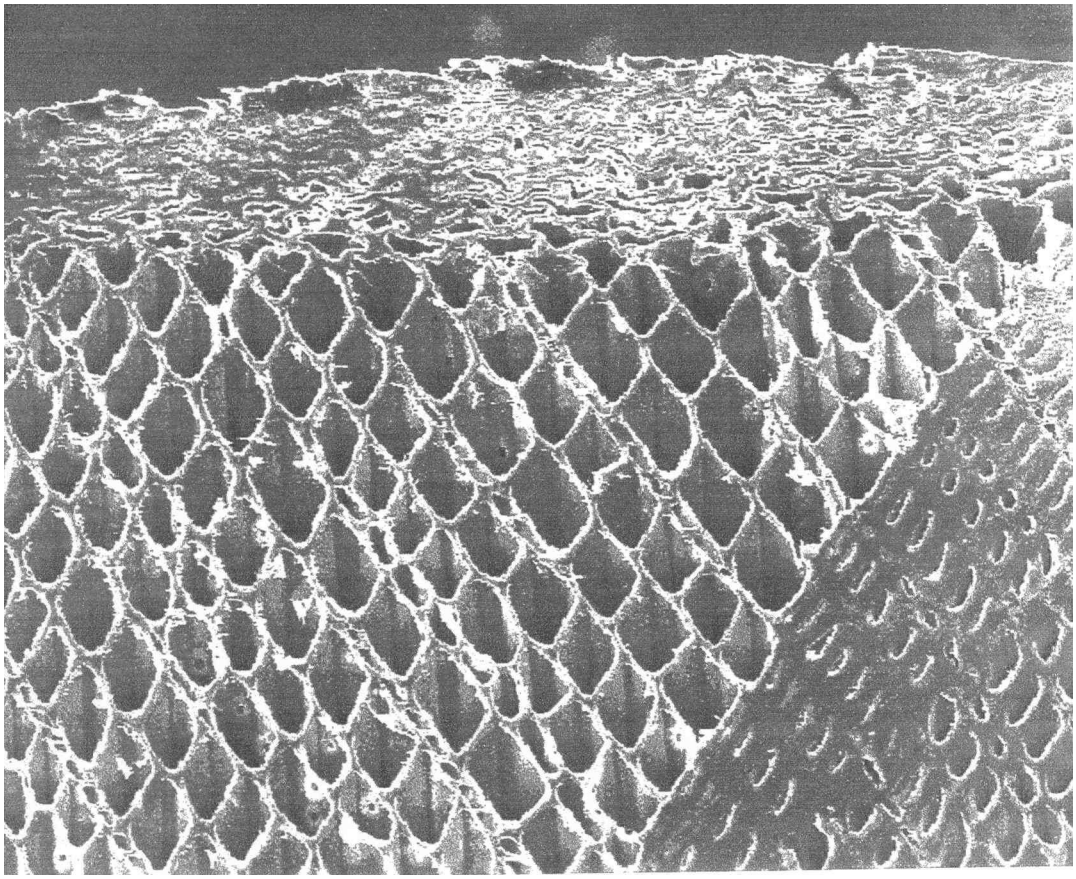

Fig. 31 Compression and permanent deformation of the surface as a result of a blunt tool edge

The permanent deformation reaches the same depth at all places; and its depth depends on the quantity of the expelled material (depth z_0 in Fig. 9).
The cell walls get essentially damaged in the compressed layer; therefore this layer loses its stability in all aspect. It will have poor mechanical strength and low abrasion resistance, humidity will cause its swelling to various extents.

Using a blunt tools edge for large-vessel wood species may result in surface waviness after compression. Oak vessels can have a diameter size up to 250-300 μm: a size where the edge of a blunt tool can fit in. In this case the edge will not only crumple but also push the material. These motions cause compression and waviness in the upper layer; the majority of the large vessels disappear from the surface due to the compression. Fig. 32 shows surface profiles of an oak probe cut with blunt and sharp-edged tools.

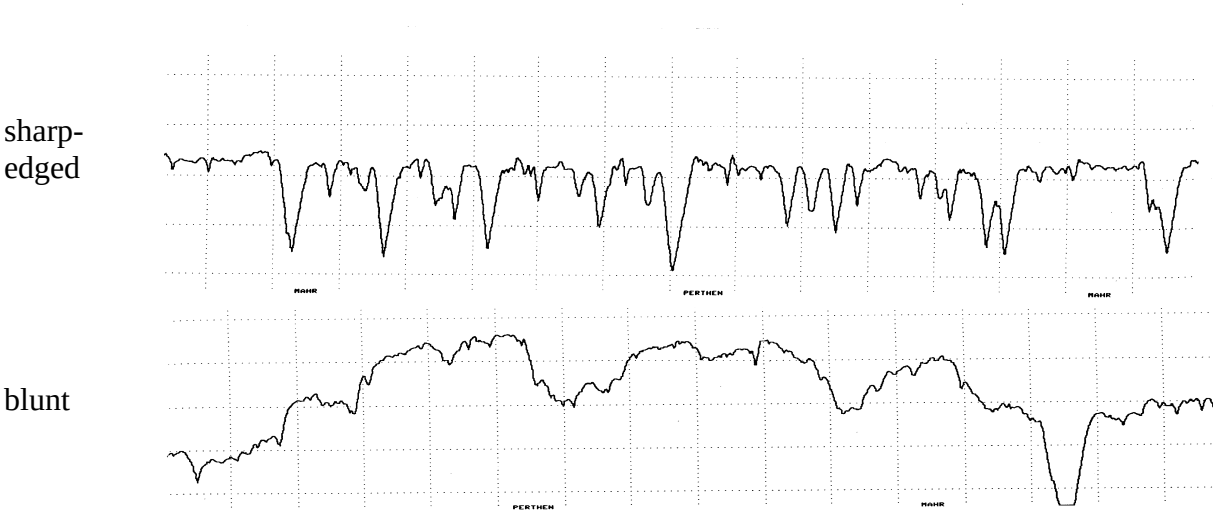

Fig. 32 Surface roughness profiles of oak machined with blunt and sharp-edged tools

When a sharp-edged tool is used, the surface is even; valleys are caused by the vessels and tracheids cut. Using a blunt tool (R=53 μm), at the same times, gives an extraordinarily wavy surface, the majority of the vessels are clogged. Consequently, the surface roughness alone is not always sufficient to characterize surface quality in every respect.

9. Scattering of roughness data

As it was established in the previous sections, the bigger part of the resultant roughness originates from the anatomical structure of wood. Cavities in the wood are cut in different angles and positions during machining, which leaves valleys on the surface. The position of the surface is accidental to the position of the vessels, early and late wood. Therefore accidental effects are also present besides deterministic effects. This is the reason for the fact that roughness parameters are always scattered around a mean value. The data scattering can be determined with a statistical method in this case, too.
Quite many, at least 50 measurement data are required for the statistical evaluation in order to ensure a normal data distribution. It is practical to plot the data with a comulated frequency

curve in a probability net, since a straight line is achieved this way. Relevant plotting for Scotch pine and oak is shown in the Figs. 33 and 34.

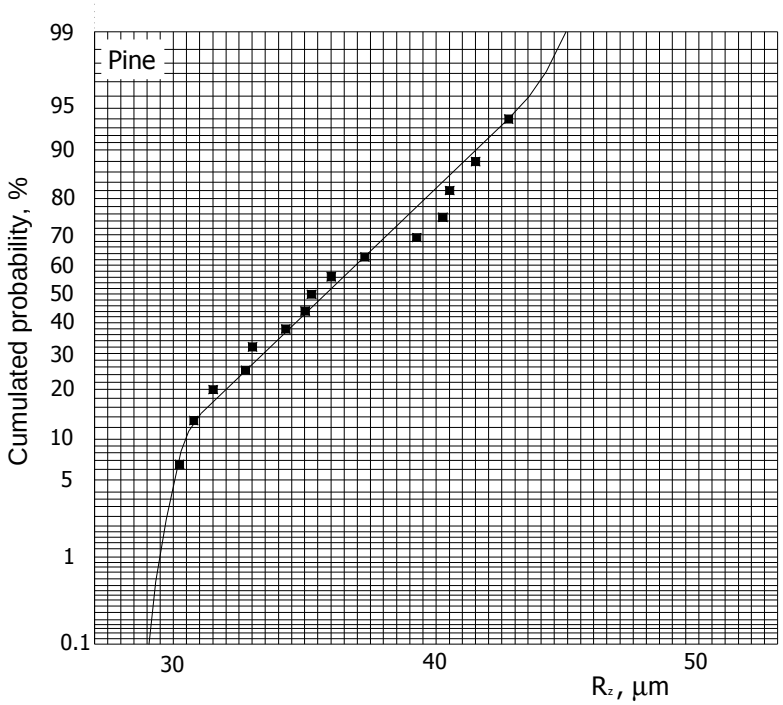

Fig. 33 Measurement data distribution in the case of a Scotch pine probe

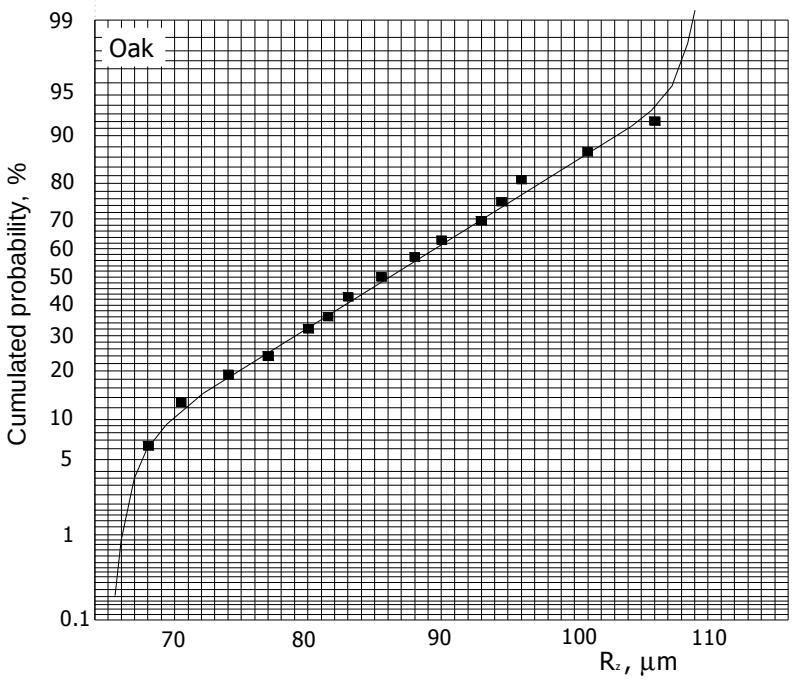

Fig. 34 Measurement data distribution in the case of an oak probe

The majority of the curves are straight with a deviation from the straight line at their ends only. This has a simple physical explanation: unlimitedly small and high values – as the

theoretical distribution would require – do not emerge in practice. Distributions like this are called uncompleted distribution
The curves clearly display the median (mean) value and the standard deviation: R_z=36±4.5 μm in the case of Scotch pine and R_z=76±12 μm in the case of oak.

Using the curves in Fig. 7 we can examine the accidental effects of early wood and late wood. The slope of the curves ($\partial\Delta F/\partial a$) describes the changeability of early wood and late wood, for a given species, which obviously influences the scattering, too. Fig. 35 shows the standard deviation of the R_z values in relation to the slope $\partial\Delta F/\partial a$ in the case of different wood species.

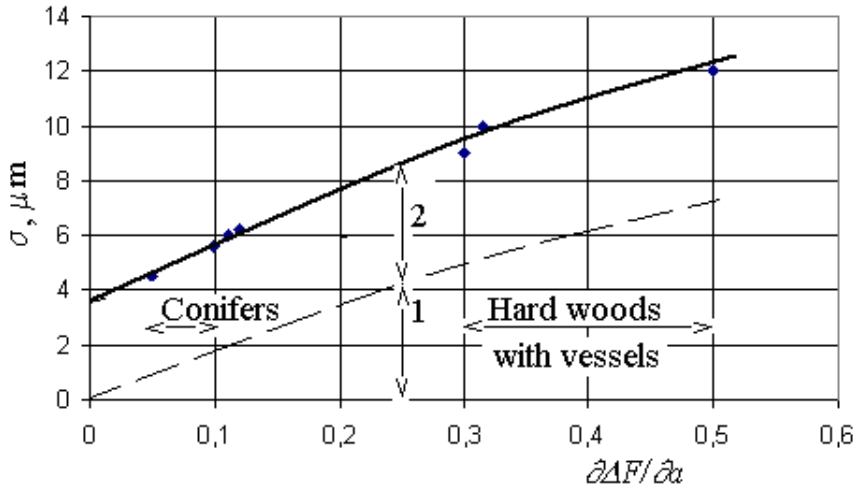

Fig. 35 Standard deviation of the roughness parameter R_z as a function of the characteristic number ∂ΔF/∂a for different wood species.
1 – component due to structural difference in early and late wood,
2 – component due to occasional placing of cutting plane to vessels

The curve is not linear but is does not significantly deviate from the straight. The intersection (σ=±3.5 μm) that belongs to the value $\partial\Delta F/\partial a=0$ theoretically corresponds with the scattering due to the accidental position of the surface relatively to the vessels and tracheids. The question is whether this value remains constant or not for all wood species. It is very likely not to remain constant; its value will increase in the case of species with large vessels.
The relative value of the standard deviation is worth examining in proportion to the mean R_z value. These test results for different wood species are shown in Table 3.

Table 3 Values of relative scattering for different wood species

Wood species	$\sigma/\overline{X}$
Scotch pine	0.13
Larch	0.14
Poplar	0.125
Beech	0.12
B. Locust	0.135
Ash	0.14
Oak	0.14

The table shows that the relative scattering of the surface roughness of different wood species is astonishingly identical; it dominantly falls in the range 0.13-0.14. In practice it makes the estimation of the standard deviation considerably easy.

10. Summary of the most important results

Investigations in the last 15 years on the main problems of the wood surface roughness brought the following new recognitions and conclusion:

- an increasing cutting speed reduces the surface roughness, firs of all by diminishing the R_{vk}-values,
- the soft wood species are more sensitive to the change of cutting velocity concerning surface roughness,
- the derived structure number is based on the sizes and specific numbers of vessels and tracheids of the wood in question, and further on the portion of early and late wood,
- the proposed structure number shows strong correlation with the attainable surface roughness,
- different roughness parameter ratios show definite correlation with the structure number. This finding further stresses the beneficial use of the structure number uniquely characterizing the different wood species.
- among the different roughness parameters interrelations are found,
- the lack of material in the rough surface can be expressed as a function of surface roughness,
- the mid component of the total roughness R_k is good indicator to predict edge dullness.
- using a special surface finishing technique, the separation of roughness components due to anatomical structure and woodworking operations has been carried out with reasonable accuracy,
- the total surface roughness can be divided into two component: the first part is the component due to machining and the second part is the component due to internal (anatomical) structure,
- in the present day practice most of the roughness is originated from the roughness component due to internal structure,
- the variation of structure number ΔF as a function of early wood portion may be quite different for the various wood species,
- using the structural properties of early and late wood, a characteristic number B can be defined which has a strong correlation with the expected relative deviation of the structure number ΔF,
- the standard deviation of the roughness parameter R_z is in strong correlation with the characteristic number $\partial\Delta F/\partial a$, while the relative value of the standard deviation practically remains constant,
- the standard deviation is originated from both the structural difference in the early and late wood and the occasional placing of cutting plane to vessels.

Literature

1. Fischer,R. und C.Schuster 1993. Zur Qualitätsentstehung spanend erzeugter Holzoberflächen. Mitteilung aus dem Institut für Holztechnik der TU Dresden.
2. Kisselbach,A. und O.Schadoffsky 1996. Gefräste Oberflächen als Eingangsgröße für die Schleifbearbeitung und Lackierung. Tagungsbericht Bielefeld.
3. Schadoffsky,O. 1996. Objektive Verfahren zur Beurteilung der Oberflächenqualität. Tagungsbericht Bielefeld.
4. Devantier,B. 1997. Prüfmethode zur objektiven Bewertung der Rauhigkeit und Welligkeit von Holzwerkstoffen. Abschlußbericht IHD Dresden.
5. Sitkei, G. et al. 1990. Theorie des Spanens von Holz. Fortschrittbericht No.1. Acta Fac. Ligniensis, Sopron.
6. Magoss, E. und Sitkei, G. 2000. Strukturbedingte Rauheit von mechanisch bearbeiteten Holzoberflächen. Möbeltage in Dresden, Tagungsbericht S. 231-239.
7. Magoss, E., G. Sitkei: Fundamental Relationships of Wood Surface Roughness at Milling Operations, Proceedings of the 15th International Wood Machining Seminar. 2001. pp. 437-446.
8. Magoss, E., G. Sitkei: Optimum Surface Roughness of Solid Woods Affected By Internal Structure and Woodworking Operations, Proceedings of the 16th International Wood Machining Seminar. 2003. pp. 366-371.
9. Magoss E., G. Sitkei und M. Lang: Allgemeine Zusammenhänge für die Rauheit von bearbeiteten Holzoberflächen für Möbel, Möbeltage in Dresden 2004.
10. A faipari műveletek elmélete, szerkesztette: Dr. Sitkei György, Mezőgazdasági Szaktudás Kiadó Kft. Budapest, 1994. (Theory of Wood Processing. Edited by G. Sitkei).
11. Csiha Csilla: Faanyagok felületi érdességének vizsgálata „P" és „R" profilon, különös tekintettel a nagyedényes fajokra, Doktori (Ph.D) értekezés, 2003. Sopron (Surface Roughness of Wood Using "P" and "R" Profiles for Big-Vessel Hardwood Species).
12. Sitkei G., On the Mechanics of Oblique Cutting of Wood. Proc. Of the 13th International Wood Machining Seminar, 1997, pp. 469-476.
13. Westkämper, E., Hofmeister, H. W., Frank, H. J.: Meßtechnisches Erfassen und Bewerten von Massivholzoberflächen. Abschlußbericht AiF Projekt 9681, Braunschweig 1996.